Case Studies in Thermal Engineering 31 (2022) 101817

Contents lists available at ScienceDirect

Case Studies in Thermal Engineering

journal homepage: www.elsevier.com/locate/csite

Grasshopper optimization algorithm for diesel engine fuelled with ethanol-biodiesel-diesel blends

Ibham Veza [a,*], Aslan Deniz Karaoglan [b,**], Erol Ileri [c], S.A. Kaulani [d], Noreffendy Tamaldin [a,***], Z.A. Latiff [e], Mohd Farid Muhamad Said [e,****], Anh Tuan Hoang [f,*****], K.V. Yatish [g], M. Idris [h]

[a] Faculty of Mechanical Engineering, Universiti Teknikal Malaysia Melaka, Hang Tuah Jaya, 76100, Durian Tunggal, Melaka, Malaysia
[b] Balikesir University, Department of Industrial Engineering, 10145, Balikesir, Turkey
[c] National Defense University, Army NCO Vocational HE School, Department of Automotive Sciences, 10110, Balıkesir, Turkey
[d] School of Mechanical Engineering, Faculty of Engineering, Universiti Teknologi Malaysia, 81310, UTM Johor Bahru, Johor, Malaysia
[e] Automotive Development Centre, Institute for Vehicle Systems and Engineering, Universiti Teknologi Malaysia, 81310, Johor Bahru, Malaysia
[f] Institute of Engineering, HUTECH University, Ho Chi Minh city, Vietnam
[g] Centre for Nano and Material Sciences, Jain University, Bangalore, Karnataka, 562112, India
[h] PT PLN (Persero), Engineering and Technology Division, Jakarta, Indonesia

GRAPHICAL ABSTRACT

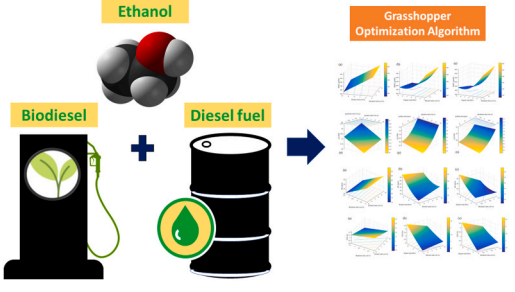

* Corresponding author.
** Corresponding author.
*** Corresponding author.
**** Corresponding author.
***** Corresponding author.
E-mail addresses: ibhamv@gmail.com (I. Veza), deniz@balikesir.edu.tr (A.D. Karaoglan), noreffendy@utem.edu.my (N. Tamaldin), mdfarid@utm.my (M.F. Muhamad Said), hatuan@hutech.edu.vn (A.T. Hoang).

https://doi.org/10.1016/j.csite.2022.101817
Received 24 November 2021; Received in revised form 6 January 2022; Accepted 20 January 2022
Available online 22 January 2022

ARTICLE INFO

Keywords:
Grasshopper optimization algorithm
Ethanol
Biodiesel
Diesel engine
Performance
Emission

ABSTRACT

A recently invented algorithm known as the grasshopper optimization algorithm (GOA) was employed to optimize diesel engine performance and emission operated with ternary fuel (ethanol-biodiesel-diesel) blends. Using the regression modelling over these experimental results; the mathematical equations between the factors i.e., ethanol ratio (vol%), biodiesel ratio (vol%), engine load (Nm)) and the responses i.e., BSFC (g/kWh), BTE (%), HC (ppm), CO_2 (%), NOx (ppm), CO (%) were calculated. Grasshopper optimization algorithm was then run through these regression equations to calculate the optimum factor levels. The confirmation results suggested that the BTE was maximized and the other responses were minimized successfully. For the ANOVA results, under the 95% confidence level with $\alpha = 5\%$ (=0.05), the p-value for all the regression models was less than 0.05, which indicated the significance of the regression models. In terms of the performance tests of the models, the regression models good fit the given observations with a low prediction error. The grasshopper optimization algorithm showed that ethanol-biodiesel-diesel blend in the ratio of 10%, 7.5%, 82.5% run at 7 Nm engine load gave the optimum results for diesel engine performance and emission characteristics. These findings have important implications for the potential of grasshopper optimization algorithm to improve engine performance and emission characteristics.

1. Introduction

Esters such as fatty methyl esters produced from virgin or used vegetable oils have been a popular choice for biodiesel production in recent years [1–3]. Another source such as *Moringa oleifera* is also a promising biodiesel feedstock [4]. Furthermore, a recent study by Sekar et al. [5] used nanocatalyst along with pyrolysis oil that was produced from plastic waste. One drawback of using esters, however, is their high viscosity that result in a number of challenges including cold starting problem [6,7]. To solve such issue, alcohol fuels such as ethanol and butanol, owing to their relatively lower viscosity, could be added to improve the overall fuel properties of biodiesel-diesel blends [8,9], thus enhancing engine performance and combustion as well as reducing harmful emissions such as smoke and particulate matter.

Mixing ethanol with diesel alone is usually known as diesohol, e-diesel, or oxygenated diesel. Owing to differences in chemical structures and physical characteristics, ethanol does not blend uniformly with diesel [10]. This is because ethanol has a hydroxyl group (OH) connected to its saturated carbon atom, enabling it to bond with H_2, thus making it a polar solvent and completely miscible with water. Note that the ethanol solubility in diesel relies on several factors such as diesel's hydrocarbon composition, temperature, water content as well as wax in the blend and humidity of the ambient condition [11]. By adding oxygenated fuel such as ethanol, the physico-chemical properties of diesel fuel will change, which later modify spray characteristics, engine performance, combustion as well as emission levels.

The majority of previous studies have reported that the alcohol addition in diesel fuel generally reduces NOx and CO emissions due to the high heat of vaporization and low C/H ratio [12,13]. Furthermore, the hydroxyl group of alcohol can improve soot oxidation, thus emitting lower soot emissions compared to diesel fuel. Despite those advantages, the addition of high percentages of alcohol in diesel engines is limited by several inferior alcohol properties such as lubricity, viscosity, cetane number and blending stability. To enhance alcohol properties, biodiesel can be added to the alcohol-diesel blend. The fatty acid methyl esters, the main compositions of biodiesel, can reduce HC, CO and soot emissions. Furthermore, just adding a small percentage of biodiesel can substantially improve the lubricity of alcohol/diesel blends. The use of ethanol-biodiesel-diesel blends is more obvious in soot emission reduction.

A number of techniques have been examined to enable the use of ethanol-diesel in diesel engines such as diesel-ethanol emulsions, dual injection and alcohol fumigation. The most common method is diesel-ethanol blends (micro-emulsion or using co-solvent) as it is considered more stable and suitable for a diesel engine without significant modifications. In their review article, Mofijur et al. [14] reported that the blends of ethanol–biodiesel–diesel had a major role in decreasing harmful emissions such as HC, CO and PM. It was recommended that around 5–10% of ethanol and 20–25% of biodiesel could be added to diesel fuel. Ghadikolaei et al. [15] investigated particulate emission of a diesel engine run with diesel-biodiesel-ethanol in fumigation and blending modes. The results showed that both modes led to alterations in micro and nano-structures of particulate matter with blended mode having lower PM emissions compared to fumigation mode.

Shamu et al. [16] examined the blends of diesel-biodiesel-ethanol running in a light-duty diesel engine. It was found that a higher concentration of ethanol gave an increased net indicated efficiency by 52% at a high engine load compared to diesel fuel, which never reached above 48%. Furthermore. The trade-off of soot-NO_X was reduced considerably using the highest ratio of ethanol. The charge cooling effect from ethanol was found to decrease the NOx emissions, while the exhaust particles also decreased both in quantity and mean diameter. At low engine loads, higher HC and CO emissions were observed for the oxygenated blends compared to the diesel fuel as the charge cooling was found to negatively affect the combustion behaviour. At higher loads, this trend was compensated due to higher in-cylinder temperature and enhanced fuel oxidation. In their studies, Noorollahi et al. [17] reported that the use D91B6E3 blend gave the best engine efficiency, performance and emission results.

Pradelle et al. [18] examined the diesel-biodiesel-ethanol as a potential blend for a Euro III engine. Specific fuel consumption was found to increase by nearly 2% for each 5 vol% addition of anhydrous ethanol. It was also reported that ethanol prolonged the ignition delay and increased the heat release rate, thus reducing the maximum pressure, which took place lately in the expansion stroke. A

minor increase in engine efficiency was also observed. In another study, Pradelle et al. [19] examined several key physico-chemical properties of diesel-biodiesel-ethanol and found that up to 20 vol% of ethanol provide enough lubricity.

Artificial computational techniques such as Artificial Neural Network (ANN) is being currently investigated extensively [20,21]. In addition to that, a recent algorithm known as the grasshopper optimization algorithm (GOA) developed by Saremi et al. [22] has attracted numerous attention. Such an optimization algorithm imitates the clusters of grasshopper behaviour to overcome optimization problems (Fig. 1). In comparison with previously established optimization algorithms, the GOA could provide better results by solving real problems with unidentified search spaces.

2. Novelty and objective of the study

Although a number of studies have shown promising results using GOA, there is no published work examining the effectiveness of the grasshopper optimization algorithm for ternary fuel such as diesel-ethanol-biodiesel blends. Hence, the objective of this study is to investigate the recently invented and effective swarm-based optimization algorithm known as GOA to optimize diesel engine performance and emission characteristics fuelled with diesel-ethanol-biodiesel blends.

In this present study, regression modelling was employed for mathematical modelling, while the GOA was used for multi-objective optimization. The GOA was used to calculate the optimum levels of factors (ethanol ratio (vol%), biodiesel ratio (vol%), and engine load (Nm) for multi-objective optimization of the responses including BSFC (g/kWh), BTE (%), HC (ppm), CO_2 (%), NOx (ppm) and CO (%).

3. Materials and methods

3.1. Experimental setup and test fuels

The experiments were performed in a single-cylinder diesel engine with its specifications and testbed setup shown in Table 1 and Fig. 2, respectively. Some devices were installed to record the data for performance and emissions measurement. These include an eddy-current brake dynamometer and an airbox having a sharp-edged orifice to quantity the air intake. The measurement for fuel consumption was performed employing a glass burette. A fuel volume of 5 ml was fixed, and the time needed to consume such an amount was measured.

The engine rotational speed was maintained at 2000 rpm, whereas the load was varied to represent various operating conditions. A gas analyser was used to measure CO, CO_2, HC and NO_x. Table 2 shows the measurement accuracy and uncertainties.

The blending technique that was employed in the present study was splash blending to facilitate better blend stability. Three diesel-ethanol-biodiesel blends were investigated namely D87.5E5B7.5, D87.5E7.5B5, and D85E10B5. Several key properties such as heating value, density and kinematic viscosity are presented in Table 3. The density was measured based on the mass and volume. The heating value was measured utilising a bomb calorimeter and the kinematic viscosity measurement was performed by means of viscometer at 40 °C, following ASTM D240 and ASTM D445, respectively.

3.2. Grasshopper optimization algorithm

Simulating nature is the foundation of meta-heuristic algorithms. These algorithms are frequently employed in the solution of global optimization problems. Meta-heuristic algorithms are classified into several types such as evolutionary-based algorithms

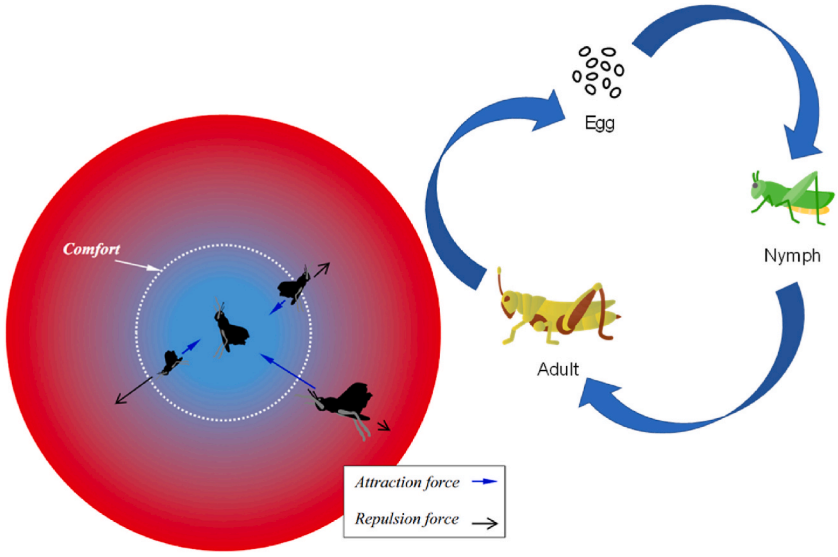

Fig. 1. Patterns of correction between individuals in a group of grasshoppers [23].

Table 1
Technical specifications of the test engine.

Description	Specification
Manufacturer	Yanmar L70 N
Type	DI, NA, 4-stroke cycle
Cooling system	Air cooling
Bore x Stroke	78 mm × 62 mm
Displacement	320 cc
Number of cylinder	1
Compression ratio	20:1
Max speed	3600 RPM
Max torque	15.69 Nm/2300 RPM
Max power	4.5 kW
Fuel injection timing	14 ± 1° before top dead centre (TDC)
Fuel injection pressure	19.6 MPa

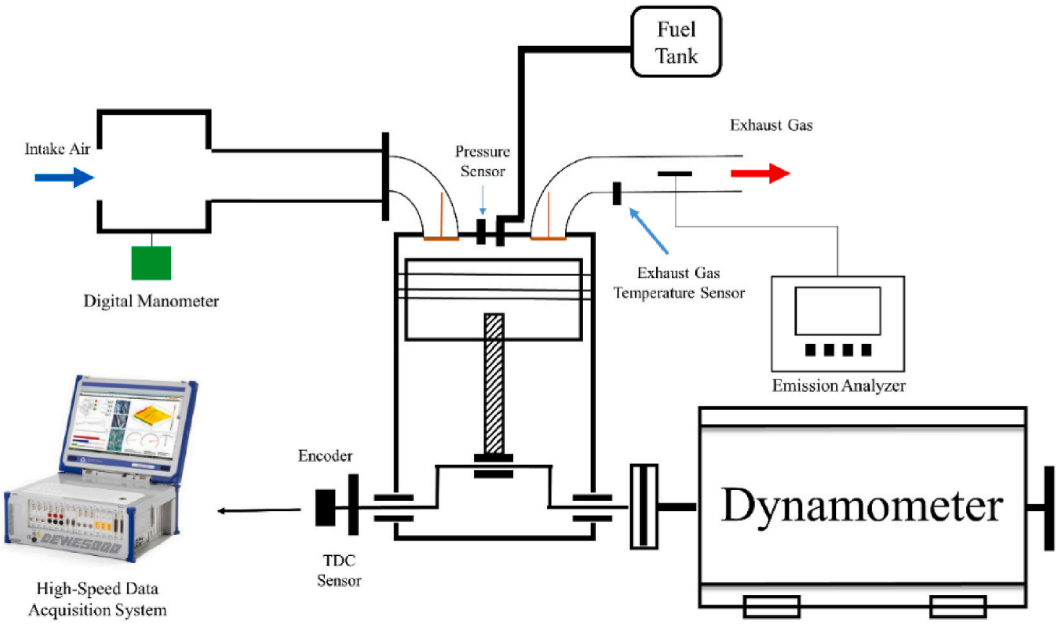

Fig. 2. The engine testbed setup.

Table 2
Measurement accuracy and uncertainties.

Instruments	Range	Accuracy	Uncertainties
HC	0–2000 ppm	±1 ppm	±4%
NO_x	0–5000 ppm	±3 ppm	±1%
CO	0–10%	±0.01%	±3%
CO^2	0–20%	±0.1%	±1%
Speed measuring unit	0–18000 rpm	±25 rpm	±2%
K type thermocouple	0–1100 °C	±0.3 °C	±0.2%
Pressure transducer	0–344.75 bar	±0.1 bar	±1%
Crank angle encoder	0–360°	±0.02°	±0.2%

Table 3
Properties of the test fuels.

Properties	Diesel	E5B7.5 D87.5[a]	E7.5B5D87.5	E10B5D85
Heating Value (MJ/kg)	45.321	43.879	43.879	42.342
Density @ 15 °C (kg/m^3)	836.13	836.75	832.42	831.53
Viscosity @ 40 °C (cSt)	4.76	4.54	4.68	4.30

[a] E5B7.5D87.5 = Ethanol 5% + Biodiesel 7.5% + Diesel 87.5%.

(genetic algorithm, etc.), swarm intelligence-based algorithms (ant colony optimization, GOA, etc.), physical & chemical based algorithms (simulated annealing, sine cosine algorithm, etc.), and human-based algorithms (harmony search, social group optimization algorithm, etc.). In this study, we used GOA for optimization. GOA is presented to the literature by Saremi et al. [22]. GOA is an effective metaheuristic algorithm that employs a swarm-based optimization inspired by nature. In this paper, GOA is used to calculate the optimum values for the input variables (optimum factor levels) those providing the maximization of BTE, while minimizing the BSFC, HC, CO_2, NOx, and CO. To perform this, the regression models those represent the numerical relation between the factors (Ethanol ratio (vol%), Biodiesel ratio (vol%), and Engine load (Nm)) and the responses (BSFC (g/kWh), BTE (%), HC (ppm), CO_2 (%), NOx (ppm), CO (%)) are calculated. Then GOA is run through these models for performing the optimization. As a result, we used GOA to search the optimum factor levels on these regression models (in other words response surfaces). The goal function for the problem is multi-objective and modelled with continuous equations.

GOA mimics grasshopper swarms' natural behaviours. Nature-inspired optimization algorithms have two phases: (*i*) exploration, and (*ii*) exploitation. In the exploration, the optimization algorithm's search agents move abruptly. However, in the exploitation, they tend to move locally. The following equations express the grasshopper's behaviours and logic of optimization search [22,24]:

$$X_i = r_1 S_i + r_2 G_i + r_3 A_i \tag{1}$$

Where i represents each grasshopper and the position of the ith grasshopper is X_i. The social interaction of the grasshoppers are represented by S_i. Similarly, gravity force and wind advection are represented by G_i, and A_i, respectively. The r terms are the random numbers between [0,1]. Social interaction of the grasshoppers (attraction-repulsion) are given in Equation (2) [22,24]:

$$S_i = \sum_{\substack{j=1 \\ j \neq i}}^{N} s\left(d_{ij}\right)\widehat{d_{ij}} \tag{2}$$

where s represents the strength of social forces ($s_r = fe^{-r/l} - e^{-r}$), l is the attractive length scale, and f is the intensity of attraction [22,24]. N denotes the number of the grasshoppers. d_{ij} is the absolute distance between ith and the jth grasshopper ($d_{ij} = |x_j - x_i|$), and $\widehat{d_{ij}}$ is a vector between two grasshoppers ($\widehat{d_{ij}} = (x_j - x_i)/d_{ij}$). The s function influences the social interaction of artificial grasshoppers. The distance between each pair of grasshoppers is divided into three sections by this function (attraction region, comfort zone, repulsion region). Saremi et al. [22] investigated distances ranging from 0 to 15, and discovered that there was repulsion between [0 2.079]. They proposed defining the comfort distance as the distance between two artificial grasshoppers separated by 2.079 units. Attraction or repulsion does not perform in the comfort zone. The f and l change this zone. If this distance is greater than 10, however, the s function returns to zero. As a summary, this result means that this function is unable to apply strong forces across long distances between grasshoppers. G_i (gravity force) is the another component of X_i [22,24]:

$$G_i = -g\widehat{e_g} \tag{3}$$

Where the gravitational constant is represented by g, and the unity vector towards the centre of the earth is represented by $\widehat{e_g}$. Finally, A_i (wind advection) is the last component of X_i:

$$A_i = u\widehat{e_w} \tag{4}$$

where u and $\widehat{e_w}$ are constant drift and unity vector in the direction of the wind, respectively. In traditional swarm-based algorithms, the swarm is simulated as exploring and exploiting the search space around a solution. In GOA, because of being the mathematical equations are in free space; the model of X_i simulates the interaction between grasshoppers in a swarm. Equation (5) is obtained by expanding Equation (1). It simulates the behaviour of the grasshopper in different space dimensions such as 2D, 3D, and hyper-dimensional spaces [22,24].

$$X_i^d = c\left(\sum_{\substack{j=1 \\ j \neq i}}^{N} c\frac{ub_d - lb_d}{2} s\left(\left|x_j^d - x_i^d\right|\right)\frac{x_j - x_i}{d_{ij}}\right) + \widehat{T_d} \tag{5}$$

The ub_d and lb_d are the upper and lower bounds in the Dth dimension s_r. $\widehat{T_d}$ is the best (target) solution, and c is the decreasing coefficient that reduces the comfort, repulsion, and attraction zones. In GOA, each search agent has a single position vector and all search agents are used to determine each search agent's following position. The first part of Equation (5) (the summation) takes other grasshoppers' positions into account and simulates grasshopper interaction. $\widehat{T_d}$ represents their tendency to move towards food sources. Finally, in Equation (6), the deceleration of grasshoppers approaching the food source is simulated by c [22,24].

$$c = cmax - l\frac{cmax - cmin}{L} \tag{6}$$

Where L and l are the maximum number of iterations and current iteration, respectively. The *cmin* and *cmax* are the minimum and maximum values [22]. In their work, Saremi et al. [22] used cmax = 1 and cmin = 0.00001, and we used the same parameters. In summary, decreasing the comfort zone by the c parameter causes the swarm to gradually converge on a stationary target. Also, the swarm properly chases a mobile target by $\widehat{T_d}$. Over the course of iterations, the grasshoppers will converge on the target. The GOA pseudo code is shown in Fig. 3 below [22].

4. Results and discussion

This study was carried out in three stages: (*i*) running the experiments, (*ii*) modelling with regression, and (*iii*) GOA optimization. Table 4 shows the levels of the factors that are used in the experimental work:

Using the factors and their levels presented in Table 3, an experimental design with 10 experimental runs were carried out and presented in Table 4. In the second stage, regression models of the responses (BSFC (g/kWh), BTE (%), HC (ppm), CO_2 (%), NOx (ppm), CO (%)) were constructed for both uncoded and coded factor levels. During the optimization phase, the coded model is required. However, to demonstrate the true mathematical relationship to the readers, the original models (the models with uncoded factor levels) were also calculated. As a result, coded factor levels are shown together with the uncoded factor levels in Table 5. Equation (7) is used to perform the coding:

$$X_{coded} = \frac{X_{uncoded} - ((X_{max} + X_{min})/2)}{(X_{max} - X_{min})/2} \tag{7}$$

The mathematical modelling was carried out in the second stage using the experimental data presented in Table 4. Equation (8) gives the representation for the full quadratic regression model:

$$Y = \beta_0 + \sum_{i=1}^{k} \beta_i X_i + \sum_{i=1}^{k} \beta_{ii} X_i^2 + \sum \sum_{i<j} \beta_{ij} X_i X_j + \varepsilon \tag{8}$$

In this equation, Y represent the response, β terms (β_0, β_i, β_{ii}, and β_{ij}) are the coefficients of the regression model, X terms (X_i: linear terms, X_i^2: quadratic terms, and X_iX_j: interaction terms) are the factors, and ε is residual terms [25–28]. Minitab, a well-known statistical package program, was used to perform regression modelling calculations and model significance tests. The original models for uncoded factor levels are presented in Equations 9–14.

$$Y_1 = +642.251697401941 + 4.71473214852899X_1 + 38.9262147169996X_2 - 84.682857991778X_3 + 8.40110204245857X_3^2 - 1.49461575614245X_1X_3 - 6.73974474435581X_2X_3 \tag{9}$$

$$Y_2 = +15.0080251985997 - 0.284883909845525X_1 - 1.51429200761536X_2 + 1.73009395973832X_3 - 0.236999829006923X_3^2 + 0.087999690243292X_1X_3 + 0.313271336193431X_2X_3 \tag{10}$$

$$Y_3 = -29.0026041666667 + 3.93333333333334X_1 + 3.59791666666668X_2 + 11.5989583333333X_3 + 0.434895833333334X_3^2 - 0.6X_1X_3 - 1.53125X_2X_3 \tag{11}$$

$$Y_4 = -2.49037202380954 + 0.217619047619048X_1 + 0.424845238095239X_2 + 1.11485119047619X_3 + 0.0109375X_3^2 - 0.050952380952381X_1X_3 - 0.091511904761905X_2X_3 \tag{12}$$

Initialize X_i, cmax, cmin, and max number of iterations
Calculate the fitness of each search agent
Assign T=the best search agent
While l<max number of iterations
  Update c by $c = cmax - l((cmax - cmin)/L)$
    For each search agent
      Normalize the d_{ij} between grasshoppers in [1,4]
      Update the position of the current search agent by X_i^d
      Bring the current search agent back if it goes outside the boundaries
    End For
  If there is a better solution **Then Update** T
  l=l+1
End While
Return T

Fig. 3. Pseudocode for Goa.

Table 4
Factor levels.

Factors	Symbols	Unit	Levels			
			1	2	3	4
Ethanol ratio	X_1	vol%	5	7.5	10	-
Biodiesel ratio	X_2	vol%	7.5	5	-	-
Engine load	X_3	Nm	3	5	7	9

Table 5
Experimental design.

Run (i)	Factors (Uncoded)			Factors (Coded)			BSFC (g/kWh)	BTE (%)	HC (ppm)	CO_2 (%)	NO_X (ppm)	CO (%)
	Ethanol (%)	Biodiesel (%)	Load (Nm)	Ethanol (%)	Biodiesel (%)	Load (Nm)						
i	X_{i1}	X_{i2}	X_{i3}	X_{i1}	X_{i2}	X_{i3}	Y_{i1}	Y_{i2}	Y_{i3}	Y_{i4}	Y_{i5}	Y_{i6}
1	5	7,5	3	−1,00	1,00	−1,00	606.89	13.79	12.00	2.40	44.00	0.06
2	5	7,5	5	−1,00	1,00	−0,33	451.12	18.56	15.00	3.00	52.33	0.07
3	5	7,5	7	−1,00	1,00	0,33	371.96	22.51	19.67	3.40	72.00	0.08
4	5	7,5	9	−1,00	1,00	1,00	354.00	23.65	26.00	4.30	88.00	0.13
5	7,5	5	3	0,00	−1,00	−1,00	558.09	15.00	20.67	2.20	36.00	0.06
6	7,5	5	5	0,00	−1,00	−0,33	435.79	19.21	26.67	2.90	44.00	0.07
7	7,5	5	9	0,00	−1,00	1,00	385.92	21.69	48.67	4.63	67.67	0.22
8	10	5	3	1,00	−1,00	−1,00	559.51	14.96	27.33	2.30	33.00	0.06
9	10	5	5	1,00	−1,00	−0,33	427.63	19.58	27.00	2.90	40.00	0.08
10	10	5	9	1,00	−1,00	1,00	364.50	22.97	45.67	4.00	68.00	0.17

$$Y_5 = +62.9813988095239 - 2.31904761904762X_1 - 2.4577380952381X_2 - 8.17410714285714X_3 + 0.463541666666666X_3^2 + 0.252380952380953X_1X_3 + 1.19107142857143X_2X_3 \quad (13)$$

$$Y_6 = -0.258981026785716 + 0.015904761904762X_1 + 0.040434226190476X_2 + 0.067874255952381X_3 + 0.003450520833333*X_3^2 - 0.003904761904762X_1X_3 - 0.010434226190476X_2X_3 \quad (14)$$

Figs. 4–9 show surface plots for the responses to help visualize the search spaces.

The MATLAB program is used for GOA coding and optimization. To use these equations in MATLAB for GOA optimization, the models had to be developed for coded factor levels ranging from −1 to 1. As a result, the models became independent of the units, and multi-objective optimization became simple [24,29–31]. Using the data in Table 4, the regression models for coded factor levels are given in Equations 15–20.

$$Y_1 = +395.245419135244 - 10.6324059708143X_1 - 1.8903171864191X_2 - 111.607968916702X_3 + 75.6099183821272X_3^2 - 11.2096181710684X_1X_3 - 25.2740427913343X_2X_3 \quad (15)$$

$$Y_2 = +20.9633019095447 + 0.607785579035576X_1 + 0.456670011931529X_2 + 4.51211861906663X_3 - 2.13299846106231X_3^2 + 0.659997676824693X_1X_3 + 1.17476751072537X_2X_3 \quad (16)$$

$$Y_3 = +23.8125 + 0.833333333333327X_1 - 6.98697916666667X_2 + 8.242187X_3 + 3.9140625X_3^2 - 4.5X_1X_3 - 5.7421875X_2X_3 \quad (17)$$

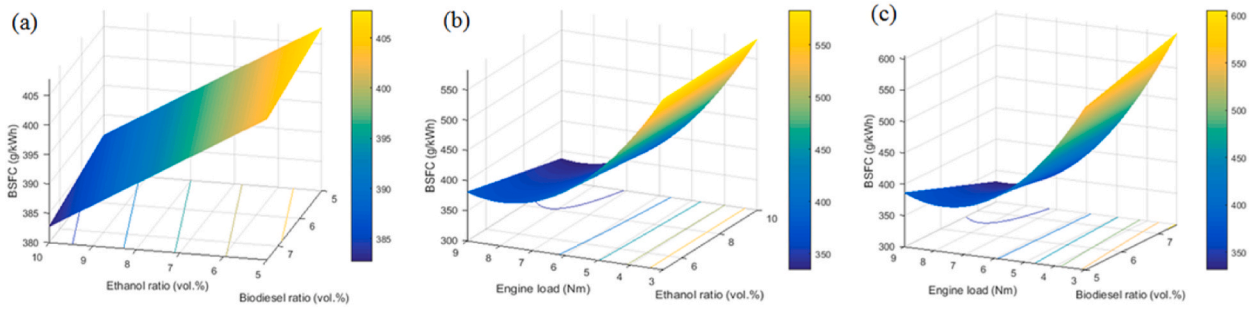

Fig. 4. Response surface plot of BSFC.

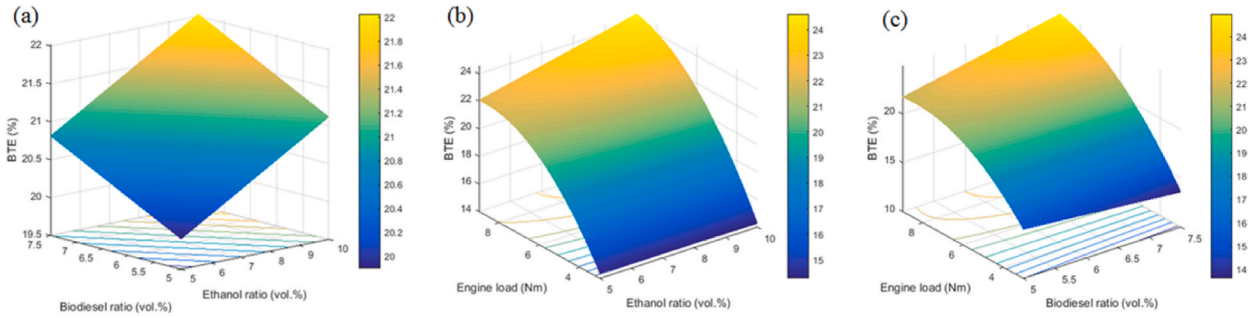

Fig. 5. Response surface plot of BTE.

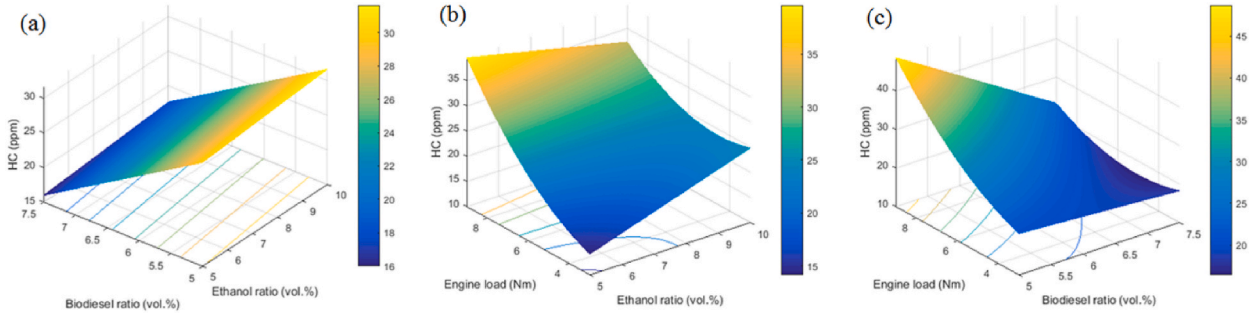

Fig. 6. Response surface plot of HC.

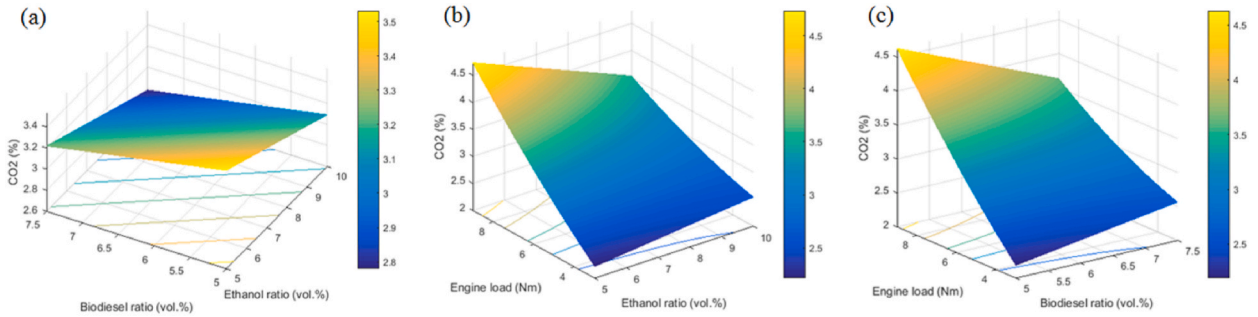

Fig. 7. Response surface plot of CO_2.

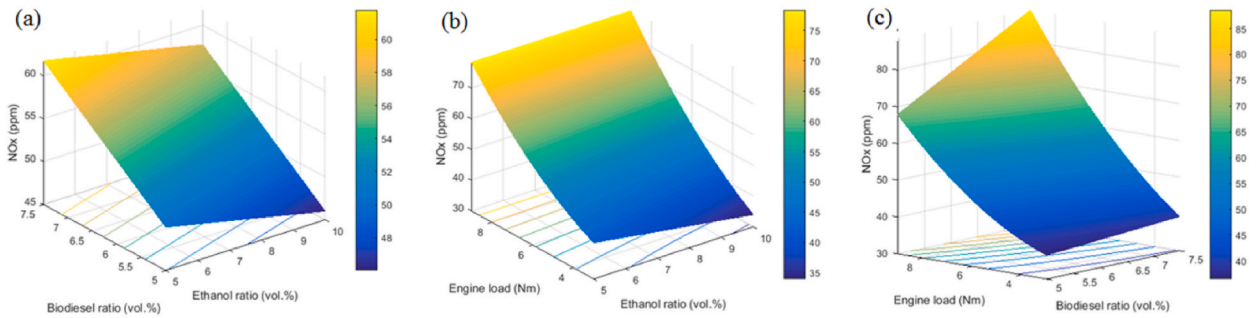

Fig. 8. Response surface plot of NOx.

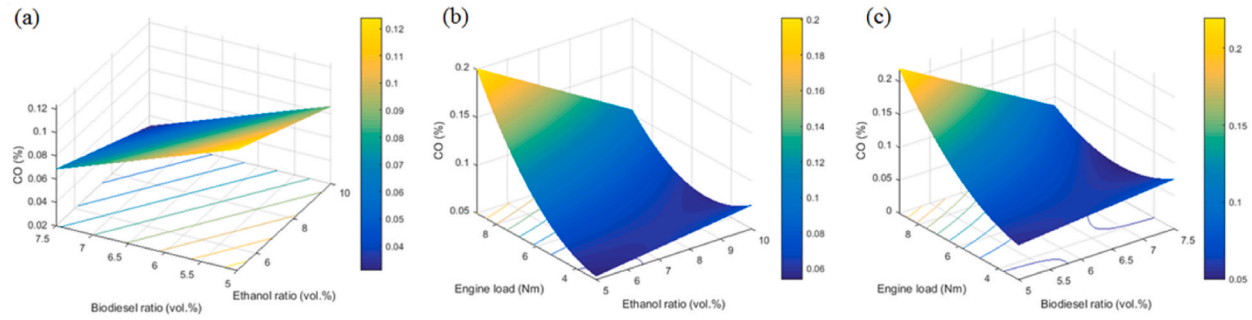

Fig. 9. Response surface plot of CO.

$$Y_4 = +3.15535714285714 - 0.220238095238096X_1 - 0.155282738095239X_2 + 0.876026785714286X_3 + 0.0984375X_3^2 - 0.382142857142857X_1X_3 - 0.343169642857143X_2X_3 \quad (18)$$

$$Y_5 = 53.8928571428571 - 2.01190476190476X_1 + 5.8608630952381X_2 + 20.1763392857143X_3 + 4.171875X_3^2 + 1.89285714285714X_1X_3 + 4.46651785714286X_2X_3 \quad (19)$$

$$Y_6 = +0.077485119047619 - 0.018809523809524X_1 - 0.027713913690476X_2 + 0.044342633928571X_3 + 0.0310546875X_3^2 - 0.029285714285714X_1X_3 - 0.039128348214286X_2X_3 \quad (20)$$

Table 6 displays the R^2 statistics associated with these models. The R^2 values must be close to 1 to use these models for optimization (which means 100%). This means the number of factors used in the model is sufficient to explain the change in the response.

The calculated R^2 values those are presented in Table 6 indicate that the ethanol ratio (X_1), biodiesel ratio (X_2) and engine load (X_3) are sufficient to model the responses and that no additional factors in the mathematical models are required. The models' significance should also be tested. The model's significance was examined using an analysis of variance (ANOVA). ANOVA is a statistical hypothesis test that employs the F-test to determine whether the regression model is significant. ANOVA has two hypotheses (null hypothesis: H_0 and alternative hypothesis: H_1). H_0 means the regression model is insignificant, while H_1 means it is significant. Therefore, to use the regression model during the optimization phase, H_1 must be true. We used the "p-value" method in this study (that is calculated by Minitab). If the p (calculated by Minitab) $<$ α (type-I error) then this means the model is significant (H_1 is true). Under the 95% confidence level with α = 5% (=0.05). The ANOVA results calculated using Minitab is given in Table 7.

According to the results displayed in Table 7, the p-value for all the regression models is less than 0.05 (5)% which means the regression models those are given in Equations 9–14 (also the same as in Equations 15–20) are significant. Table 8 displays the results of the mathematical models. According to this table, observed responses (experimental results) are represented by Y_i, while Minitab results are the expected results and represented by $\widehat{Y}_i$. These expected results namely $\widehat{Y}_i$ are calculated using the fitted regression equation. PE_i is the prediction error of the i*th* run calculated using the formula given in Equation (21) below:

$$PE_i(\%) = 100\frac{|Y_i - \widehat{Y}_i|}{\widehat{Y}_i} \quad (21)$$

According to the results presented in Table 8, it can be concluded that the regression models good fit the given observations with a low prediction error (PE). In the third stage, the MATLAB programme was used for coding GOA and performing the optimization [8,9]. In the algorithm, it is decided to use 100 search agents. In addition, the maximum number of iterations is determined as 200. The number of search agents and the number of iterations were determined by referring to the literature and through a set of preliminary experiments. The problem was modelled as a constrained continuous optimization problem [9,14–16]. For this purpose, the regression models given in Equations 15–20 were used and then the GOA algorithm was run through this model under the given constraint to optimize the factors.

$$Z = +\left|Y_{1,coded}/\max(Y_{i1})\right| - \left|Y_{2,coded}/\max(Y_{i2})\right| + \left|Y_{3,coded}/\max(Y_{i3})\right| + \left|Y_{4,coded}/\max(Y_{i4})\right| + \left|Y_{5,coded}/\max(Y_{i5})\right| + \left|Y_{6,coded}/\max(Y_{i6})\right| \quad (22)$$

Table 6
Table for calculated coefficient of determination values.

Coefficient of Determination	Responses					
	Y_1	Y_2	Y_3	Y_4	Y_5	Y_6
R^2 (%)	99.98	99.82	99.3	99.42	99.58	98.79
R^2 (prediction) (%)	99.69	98.8	79.8	91.69	96.25	68.25
R^2 (adjusted) (%)	99.93	99.45	97.91	98.27	98.74	96.36

Table 7
ANOVA results.

Response	P-Value vs Alpha	Result
BSFC	0.000 < 0.05	Model Significant
BTE	0.000 < 0.05	Model Significant
HC	0.003 < 0.05	Model Significant
CO_2	0.002 < 0.05	Model Significant
NOx	0.001 < 0.05	Model Significant
CO	0.006 < 0.05	Model Significant

Table 8
Performance tests of the models.

Run (i)	BSFC (g/kWh)			BTE (%)			HC (ppm)		
	Y_{i1}	$\widehat{Y}_{i1}$	PE_{i1} (%)	Y_{i2}	$\widehat{Y}_{i2}$	PE_{i2} (%)	Y_{i3}	$\widehat{Y}_{i3}$	PE_{i3} (%)
1	606.89	605.2698	0.27	13.79	13.6523	1.04	12.00	12.9063	7.02
2	451.12	454.2794	0.70	18.56	18.8996	1.81	15.00	14.0938	6.43
3	371.96	370.4978	0.40	22.51	22.2508	1.15	19.67	18.7604	4.83
4	354.00	353.9250	0.02	23.65	23.7061	0.24	26.00	26.9063	3.37
5	558.09	559.0796	0.18	15.00	15.0363	0.24	20.67	20.7292	0.30
6	435.79	434.3148	0.34	19.21	19.1572	0.28	26.67	26.5729	0.35
7	385.92	386.4117	0.13	21.69	21.7110	0.08	48.67	48.6979	0.06
8	559.51	559.6568	0.03	14.96	14.9841	0.14	27.33	26.0625	4.88
9	427.63	427.4189	0.05	19.58	19.5450	0.16	27.00	28.9063	6.59
10	364.50	364.5697	0.02	22.97	22.9788	0.05	45.67	45.0313	1.41
Run (i)	CO_2 (%)			NOx (ppm)			CO (%)		
	Y_{i4}	$\widehat{Y}_{i4}$	PE_{i4} (%)	Y_{i5}	$\widehat{Y}_{i5}$	PE_{i5} (%)	Y_{i6}	$\widehat{Y}_{i6}$	PE_{i6} (%)
1	2.40	2.4038	0.16	44.00	43.1875	1.88	0.06	0.0651	7.88
2	3.00	2.9263	2.52	52.33	54.6458	4.23	0.07	0.0605	15.64
3	3.40	3.5363	3.85	72.00	69.8125	3.13	0.08	0.0835	4.23
4	4.30	4.2338	1.56	88.00	88.6875	0.78	0.13	0.1341	0.60
5	2.20	2.1899	0.46	36.00	36.4940	1.35	0.06	0.0528	13.67
6	2.90	2.9152	0.52	44.00	43.2589	1.71	0.07	0.0808	13.39
7	4.63	4.6283	0.11	67.67	67.9137	0.36	0.22	0.2197	1.64
8	2.30	2.3518	2.20	33.00	32.5893	1.26	0.06	0.0633	5.15
9	2.90	2.8223	2.75	40.00	40.6161	1.52	0.08	0.0718	6.81
10	4.00	4.0259	0.64	68.00	67.7946	0.30	0.17	0.1716	0.95

$$\text{Min Z s.t. } X_1 \in [-1,1];\ X_2 \in [-1,1];\ X_3 \in [-1,1] \tag{23}$$

Note that the signs given in the equation of Z have to be " − " for maximization and " + " for minimization at GOA MATLAB code (see Ref. [9] for details). The max (Y_i) values are the maximum observed values of each response at the experimental design given in Table 4. The CPU time is calculated as 53.18 s at a PC with a processor with Intel i5 2.4 GHz - 4 GB RAM. GOA calculated the optimized factor levels as $X_1 = 10$ (coded value: 1), $X_2 = 7.5$ (coded value: 1) and $X_3 = 6.98$ (coded value: 0.3253). Because X3 = 6.98 is an invalid value, it has been rounded to the nearest integer number and recalculated as 7. For this optimized factor level combination, the confirmation results are presented in Table 9:

5. Conclusions

By employing regression modelling from the experimental results; the mathematical equations between the factors (ethanol ratio

Table 9
Confirmation for the optimized factor levels.

Optimized responses	Y_i	$\widehat{Y}_i$	PE_i (%)
BSFC (g/kWh)	341.23	342.54	0.38
BTE (%)	23.6494	23.8667	0.91
HC (ppm)	16.6683	17.4224	4.33
CO_2 (%)	2.7707	2.8393	2.42
NOx (ppm)	65.72	66.81	1.63
CO (%)	0.0247	0.0264	6.44

(vol%), biodiesel ratio (vol%), engine load (Nm)) and the responses (BSFC (g/kWh), BTE (%), HC (ppm), CO_2 (%), NOx (ppm), CO (%)) were calculated. The following conclusions can be drawn from the present study:

i. The ethanol ratio (X_1), biodiesel ratio (X_2) and engine load (X_3) were found to be sufficient to model the responses with no additional factors required in the mathematical models.
ii. For the ANOVA results, Under the 95% confidence level with $\alpha = 5\%$ (=0.05), the p-value for all the regression models was less than 0.05, which indicated the significance of the regression models in the present study. In terms of the performance tests of the models, the regression models good fit the given observations with a low prediction error (PE).
iii. The Grasshopper optimization algorithm showed that the ethanol-biodiesel-diesel blend in the ratio of 10%, 7.5%, 82.5% run at 7 Nm engine load gave the optimum results for diesel engine performance and emission characteristics performed in this study.

All in all, the results of this study indicate the potential of a grasshopper algorithm for multi objective-optimization of diesel engine fuelled with ternary fuel such as ethanol-biodiesel-diesel blends. However, further work is required to establish the viability of grasshoppers optimization algorithm for ICE application. This include incorporating the combustion data, such as in-cylinder pressure, heat release rate and pressure rise rate for a more comprehensive analysis.

CRediT authorship contribution statement

Ibham Veza: Conceptualization, Methodology, Validation. **Aslan Deniz Karaoglan:** Investigation, Writing – original draft. **Erol Ileri:** Formal analysis, Writing – original draft, Visualization. **S.A. Kaulani:** Resources. **Noreffendy Tamaldin:** Supervision, Funding acquisition. **Z.A. Latiff:** Resources, Supervision. **Mohd Farid Muhamad Said:** Supervision, Funding acquisition. **Anh Tuan Hoang:** Writing – review & editing. **K.V. Yatish:** Writing – review & editing. **M. Idris:** Project administration.

Declaration of competing interest

The authors declare that they have no known competing financial interests or personal relationships that could have appeared to influence the work reported in this paper.

Acknowledgement

The authors would like to acknowledge the Universiti Teknologi Malaysia (UTM) and Universiti Teknikal Malaysia Melaka (UTeM) for the university research grant Q.J130000.3509.06G97 and postdoctoral fellowship, respectively.

References

[1] S. Rajendran, A comparative study of performance and emission characteristics of neat biodiesel operated diesel engine: a review, J. Therm. Anal. Calorim. 146 (3) (2021) 1015–1025.
[2] R. Senthil, G. Pranesh, R. Silambarasan, Leaf extract additives: A solution for reduction of NOx emission in a biodiesel operated compression ignition engine, Energy 175 (2019) 862–878.
[3] S.K. Nayak, S. Nižetić, V.V. Pham, Z. Huang, A.I. Ölçer, V.G. Bui, et al., Influence of injection timing on performance and combustion characteristics of compression ignition engine working on quaternary blends of diesel fuel, mixed biodiesel, and t-butyl peroxide. doi:10.1016/j.jclepro.2021.130160.
[4] B. Kanimozhi, G. kumar, M. Alsehli, A. Elfasakhany, D. Veeman, S. Balaji, et al., Effects of oxyhydrogen on the CI engine fueled with the biodiesel blends: A performance, combustion and emission characteristics study, Int. J. Hydrogen Energy (2021).
[5] M. Sekar, T.R. Praveenkumar, V. Dhinakaran, P. Gunasekar, A. Pugazhendhi, Combustion and emission characteristics of diesel engine fueled with nanocatalyst and pyrolysis oil produced from the solid plastic waste using screw reactor, J. Clean. Prod. 318 (2021) 128551.
[6] I. Veza, V. Muhammad, R. Oktavian, D.W. Djamari, M.F.M. Said, Effect of COVID-19 on biodiesel industry: A case study in Indonesia and Malaysia, Int. J. Automot. Mech. Eng. 18 (2) (2021) 8637–8646.
[7] M. Rusli, M.M. Said, A. Sulaiman, M. Roslan, I. Veza, M.M. Perang, et al., Performance and emission measurement of a single cylinder diesel engine fueled with palm oil biodiesel fuel blends, IOP Conference Series: Materials Science and Engineering. 1068. IOP Publishing (2021) 12020.
[8] I. Veza, M. Faizullizam Roslan, Farid Muhamad Said M, abdul latiff Z, azman abas M. Physico-chemical properties of Acetone-butanol-ethanol (ABE)-diesel blends: blending strategies and mathematical correlations, Fuel 286 (2021) 119467.
[9] I. Veza, M.F.M. Said, Z.A. Latiff, Recent advances in butanol production by acetone-butanol-ethanol (ABE) fermentation, Biomass Bioenergy 144 (2021) 105919.
[10] N. Ganesan, T.H. Le, P. Ekambaram, D. Balasubramanian, V.V. Le, A.T. Hoang. Experimental assessment on performance and combustion behaviors of reactivity-controlled compression ignition engine operated by n-pentanol and cottonseed biodiesel. doi:10.1016/j.jclepro.2021.129781.
[11] G. Labeckas, S. Slavinskas, M. Mažeika, The effect of ethanol–diesel–biodiesel blends on combustion, performance and emissions of a direct injection diesel engine, Energy Convers. Manag. 79 (2014) 698–720.
[12] I. Veza, M.F.M. Said, Z.A. Latiff, Progress of acetone-butanol-ethanol (ABE) as biofuel in gasoline and diesel engine: A review, Fuel Process. Technol. 196 (2019) 106179.
[13] I. Veza, M.F.M. Said, Z.A. Latiff, Improved performance, combustion and emissions of SI engine fuelled with butanol: A review, Int. J. Automot. Mech. Eng. 17 (1) (2020) 7648–7666.
[14] M. Mofijur, M.G. Rasul, J. Hyde, A.K. Azad, R. Mamat, M.M.K. Bhuiya, Role of biofuel and their binary (diesel–biodiesel) and ternary (ethanol–biodiesel–diesel) blends on internal combustion engines emission reduction, Renew. Sustain. Energy Rev. 53 (2016) 265–278.
[15] M.A. Ghadikolaei, L. Wei, C.S. Cheung, K.-F. Yung, Z. Ning, Particulate emission and physical properties of particulate matter emitted from a diesel engine fueled with ternary fuel (diesel-biodiesel-ethanol) in blended and fumigation modes, Fuel 263 (2020) 116665.
[16] S. Shamun, G. Belgiorno, G. Di Blasio, C. Beatrice, M. Tunér, P. Tunestål, Performance and emissions of diesel-biodiesel-ethanol blends in a light duty compression ignition engine, Appl. Therm. Eng. 145 (2018) 444–452.
[17] Y. Noorollahi, M. Azadbakht, B. Ghobadian, The effect of different diesterol (diesel–biodiesel–ethanol) blends on small air-cooled diesel engine performance and its exhaust gases, Energy 142 (2018) 196–200.
[18] F. Pradelle, S. Leal Braga, A.R. Fonseca de Aguiar Martins, F. Turkovics, R. Nohra Chaar Pradelle, Performance and combustion characteristics of a compression ignition engine running on diesel-biodiesel-ethanol (DBE) blends – potential as diesel fuel substitute on an Euro III engine, Renew. Energy 136 (2019) 586–598.
[19] F. Pradelle, S. Leal Braga, A.R. Fonseca de Aguiar Martins, F. Turkovics, R. Nohra Chaar Pradelle, Experimental assessment of some key physicochemical properties of diesel-biodiesel-ethanol (DBE) blends for use in compression ignition engines, Fuel 248 (2019) 241–253.

[20] I. Veza, M.F. Roslan, M.F.M. Said, Z.A. Latiff, M.A. Abas, Cetane index prediction of ABE-diesel blends using empirical and artificial neural network models, Energy Sources, Part A Recovery, Util. Environ. Eff. (2020) 1–18.
[21] I. Veza, M.F. Muhamad Said, Z. Abdul Latiff, M.A. Abas, Application of Elman and Cascade neural network (ENN and CNN) in comparison with adaptive neuro fuzzy inference system (ANFIS) to predict key fuel properties of ABE-diesel blends, Int. J. Green Energy (2021) 1–13.
[22] S. Saremi, S. Mirjalili, A. Lewis, Grasshopper optimisation Algorithm: theory and application, Adv. Eng. Software 105 (2017) 30–47.
[23] I. Aljarah, A.-Z. Ala'M, H. Faris, M.A. Hassonah, S. Mirjalili, H. Saadeh, Simultaneous feature selection and support vector machine optimization using the grasshopper optimization algorithm, Cognitive Computation 10 (3) (2018) 478–495.
[24] S. Mirjalili, Grasshopper optimisation algorithm, Available from: https://seyedalimirjalili.com/, 2020. (Accessed 1 June 2021).
[25] D.C. Montgomery, Design and analysis of experiments, John wiley & sons (2017).
[26] E. Ileri, A.D. Karaoglan, A. Atmanli, Response surface methodology based prediction of engine performance and exhaust emissions of a diesel engine fuelled with canola oil methyl ester, J. Renew. Sustain. Energy 5 (3) (2013), 033132.
[27] A. Atmanlı, B. Yüksel, E. Ileri, A.D. Karaoglan, Response surface methodology based optimization of diesel–n-butanol–cotton oil ternary blend ratios to improve engine performance and exhaust emission characteristics, Energy Convers. Manag. 90 (2015) 383–394.
[28] N. Yilmaz, E. Ileri, A. Atmanlı, A. Deniz Karaoglan, U. Okkan, M. Sureyya Kocak, Predicting the engine performance and exhaust emissions of a diesel engine fueled with hazelnut oil methyl ester: the performance comparison of response surface methodology and LSSVM, J. Energy Resour. Technol. (2016) 138 (5).
[29] E. Ileri, A.D. Karaoglan, S. Akpinar, Optimizing cetane improver concentration in biodiesel-diesel blend via grey wolf optimizer algorithm, Fuel 273 (2020) 117784.
[30] A.D. Karaoglan, Optimizing plastic extrusion process via grey wolf optimizer Algorithm and regression Analysis, J. Sci. Ind. Res. 80 (1) (2021) 34–41.
[31] A.D. Karaoglan, B. Baydeniz, Optimizing plastic injection process using whale optimization Algorithm in automotive lighting parts manufacturing, J. Sci. Ind. Res. 80 (4) (2021) 360–368.